Journal of Advanced Research in Applied Sciences and Engineering Technology

Journal homepage:
https://semarakilmu.com.my/journals/index.php/applied_sciences_eng_tech/index
ISSN: 2462-1943

Investigation of Electromechanical Characteristics of a Three-Phase Linear Generator

Rajendran Sinnadurai[1,*], Devika Sethu[2], Rohaizah Mohd Ghazali[1], Siti Nor Baizura Zawawi[1], Viveghen Emanuel Velan P. Wilson[1]

[1] Department of Electrical Engineering, Faculty of Engineering and Life Sciences, University of Selangor, Bestari Jaya Campus, Selangor, Malaysia
[2] Electronics Engineering, Manipal International University Nilai, Negeri Sembilan, Malaysia

ARTICLE INFO

Article history:
Received 17 May 2023
Received in revised form 13 September 2023
Accepted 20 September 2023
Available online 6 October 2023

Keywords:
D-Q synchronous inductance; power; Maximum Torque Per Ampere; MTPA; saliency

ABSTRACT

The motion of sea waves can be converted into electrical energy using a three-phase linear generator. This paper investigates the electromechanical characteristics of two types of the three-phase linear generator, namely TPLG-6 and TPLG-18. The electromechanical characteristics such as power, efficiency, torque, d-q axis synchronous inductance, saliency ratio and current are investigated. MATLAB Simulink is used for the simulation. In this study, the d-q synchronous inductance is calculated to investigate the effects of d-q synchronous inductance on the permanent magnet. The Maximum Torque Per Ampere (MTPA) is plotted to determine the torque required to generate the maximum d-q current. The saliency ratio will also be investigated by comparing the d-q synchronous inductance for TPLG-6 and TPLG-18.

1. Introduction

A linear generator is an electromechanical device that generates electricity using sea wave energy. The linear generator is lighter and more compact because there is no rotating part. Unlike rotating generators that rotate, the linear generator moves in a linear motion so that when it hits an endpoint, it stops and moves in the opposite direction. The two essential parts of a linear generator are the stator and the translator. The stator consists of three-phase windings and a nonlinear magnetic core, while the translator consists of a shaft with permanent magnets, each separated by nonlinear magnetic materials [1,2,14]. This study investigates the electromechanical characteristics of two types of three-phase linear generators, the TPLG-6 and the TPLG-18. The TPLG-6 and the TPLG-18 consist of 6 and 18 slots, respectively [7].

In recent years, there has been significant growth in electrical generation worldwide, which is anticipated to persist. Therefore, developing an energy-efficient generator has been a major task for engineers and researchers. Moreover, higher efficiency has been proven to reduce electricity consumption [3,18,20]. Conventional energy sources mainly contribute the electricity generation in

* *Corresponding author.*
E-mail address: rajendran@unisel.edu.my

https://doi.org/10.37934/araset.32.3.228240

Malaysia. Although conventional energy sources can produce a significant amount of energy, they cause significant harm to the environment, especially greenhouse gas emissions and other disadvantages, such as health problems for humans and animals [19]. As our country still generates electricity by burning fuel and gas, Malaysia is estimated to release 285.73 million tons of CO_2 by 2020, an increase of 68.86% from the amount of CO_2 emitted in 2000 [4,5,17].

Besides the environmental impacts, high operating and maintenance costs are also the compelling reason for shifting to unconventional energy sources such as sea waves. Linear generator with radial permanent magnets is a well-known sea wave energy converting device, providing high linear force and efficiency [5]. In order to extract this massive sea waves energy, various Wave Energy Converter (WEC) devices have been proposed, such as Archimedes Wave Swing (AWS), LIMPET, Pelamis, Wave Dragon and Electroactive Polymer Artificial Muscles (EPAM) [6,7,10,11,16]. However, most of these devices were offshore, leading to high maintenance costs. On top of that, these devices have low efficiency since they use hydraulic systems and turbines as their Power-Take-Off [15]. The linear movement of the generator has a significant problem known as a cogging force when it stops at an endpoint. In this study, the efficiency of three-phase linear generators are to be investigated.

2. Park's Transformation

The TPLG can be placed in the d-q frame by applying the park transformation. The park's transformation is computed by multiplying the ABC or αβ components with a matrix set that converts time-varying elements into time-invariant elements. The d-q reference is useful to denote the direct axis aligned with the direction of magnetic flux, Ψ_m or Ψ_f, as shown in Figure 1; meanwhile, the q-axis bisects the part of the PMs at the translator [12].

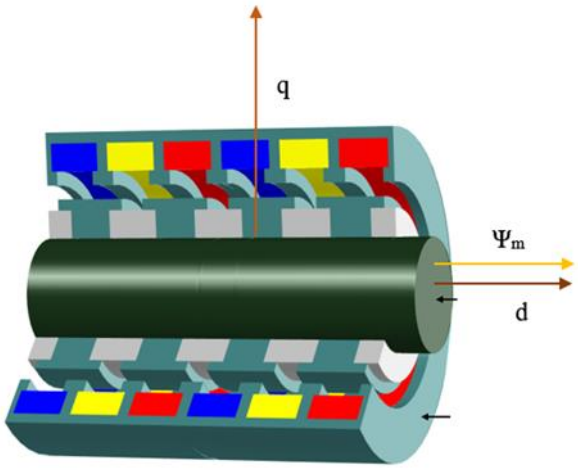

Fig. 1. Direct Quadrature Frame of a Linear Generator

The current induced in the q direction in the d-q reference would create a magnetomotive force known as the torque current, LQ. The current in the d direction is known as the field current, Id. Positive Id current helps magnet flux to create more magnetic flux, but it is important to avoid exceeding the saturation point of iron. Negative Id currents decrease the magnet flux, weakening the magnetic field. Saliency occurs in the PMs Machine when the stator current reaches the preferred magnetic direction [8].

The stator inductance is not a function of translator position and was kept constant as calculated by injecting rated currents of about 43.44 A and 21.28 A for TPLG-18 and TPLG-6, respectively [7,9].

The stator voltage was calculated as a function of stator resistance, current, and rate of change of magnetic flux using Eq. (1).

$$\begin{bmatrix} V_{as} \\ V_{bs} \\ V_{cs} \end{bmatrix} = \begin{bmatrix} rs & 0 & 0 & 0 & 0 & 0 \\ 0 & rs & 0 & 0 & 0 & 0 \\ 0 & 0 & rs & 0 & 0 & 0 \end{bmatrix} \begin{bmatrix} I_{as} \\ I_{bs} \\ I_{cs} \end{bmatrix} + \frac{d}{dt} \begin{bmatrix} \lambda_{as} \\ \lambda_{bs} \\ \lambda_{cs} \end{bmatrix} \quad (1)$$

The Eq. (2) and Eq. (3) are used to transform the ABC values to d-q values [13].

$$\begin{bmatrix} V_{ds} \\ V_{qs} \\ V_{0s} \end{bmatrix} = \frac{2}{3} \begin{bmatrix} \cos\theta & \cos(\theta - 120^0) & \cos(\theta + 120^0) \\ \sin\theta & \sin(\theta - 120^0) & \sin(\theta + 120^0) \\ \frac{1}{2} & \frac{1}{2} & \frac{1}{2} \end{bmatrix} \begin{bmatrix} V_{as} \\ V_{bs} \\ V_{cs} \end{bmatrix} \quad (2)$$

$$\begin{bmatrix} i_{ds} \\ i_{qs} \\ i_{0s} \end{bmatrix} = \frac{2}{3} \begin{bmatrix} \cos\theta & \cos(\theta - 120^0) & \cos(\theta + 120^0) \\ \sin\theta & \sin(\theta - 120^0) & \sin(\theta + 120^0) \\ \frac{1}{2} & \frac{1}{2} & \frac{1}{2} \end{bmatrix} \begin{bmatrix} I_{as} \\ I_{bs} \\ I_{cs} \end{bmatrix} \quad (3)$$

The flux linkage, in terms of d-q, is computed using Eq. (4) and Eq. (5).

$$\lambda_{qs} = \left(L_{as} + \frac{3}{2}L_m\right) I_{qs} + \left(\frac{3}{2}L_m I_{qr}\right) \quad (4)$$

$$\lambda_{ds} = \left(L_{as} + \frac{3}{2}L_m\right) I_{ds} + \left(\frac{3}{2}L_m I_{dr}\right) \quad (5)$$

The d-q synchronous inductances are computed using Eq. (6) and Eq. (7).

$$L_d = \frac{\Psi_d}{i_d} \quad (6)$$

$$L_{dq} = \frac{\Psi_q}{i_q} \quad (7)$$

The electromagnetic torque developed is calculated by Eq. (8).

$$T_{magnetic} = \frac{3p}{2}\left[i_d i_q \left(L_d - L_q\right) + \Psi_d i_d\right] \quad (8)$$

3. D-Q Simulation

Figure 2 shows the overall simulation process according to the equations.

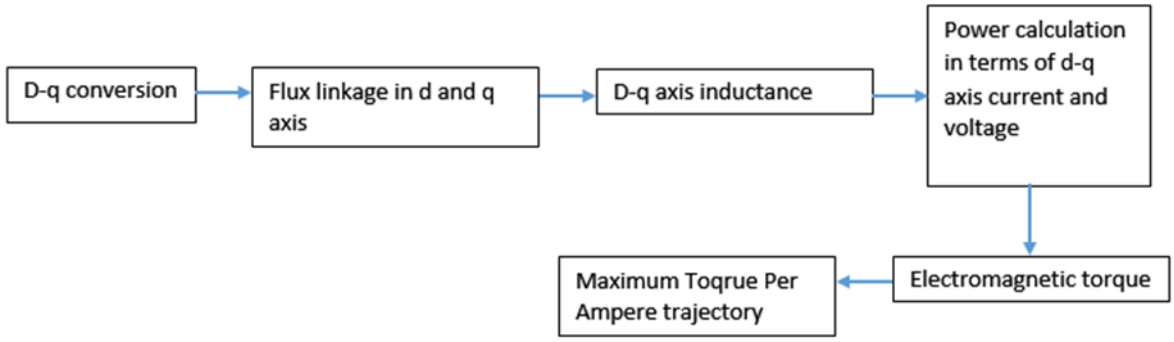

Fig. 2. Overall simulation flow

MATLAB Simulink is used for the d-q simulation, as shown in Figure 3. The simulation starts with an input of ideal sinusoidal voltage and current waveforms to be converted into d-q values. These d-q currents, id and iq are then used to compute the flux linkage of the d and q axes, respectively. From the average flux linkage, in d-q axes, the d-q synchronous inductance is computed using Eq. (6) and Eq. (7). Finally, the electromagnetic torque is computed as a function of d-q synchronous inductance, current, power and d-axis flux linkage as in Eq. (8).

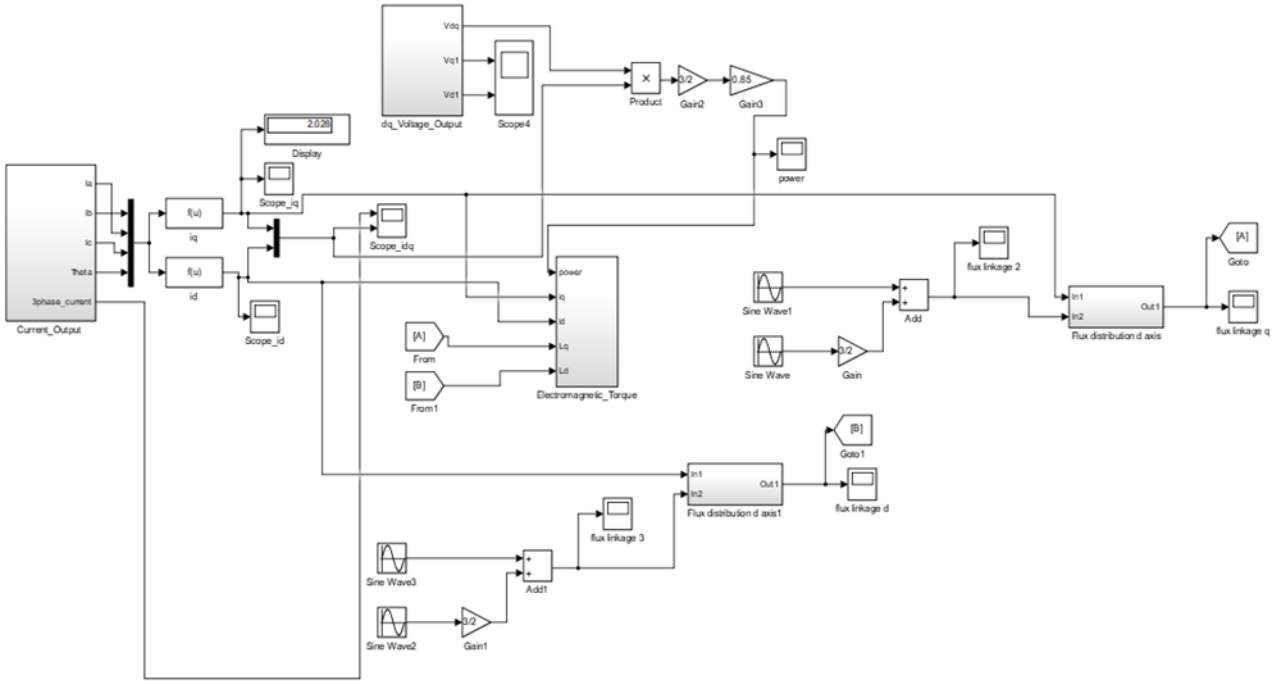

Fig. 3. Simulation of d-q block

The generator is expected to deliver three ideal sinusoidal input voltages as it performs under dynamic conditions. The output voltage of TPLG-6 and TPLG-18 are 162V and 512.2V, respectively. Similarly, for output current for the dynamic condition [7,9]. Figure 4 depicts the ideal sinusoidal input current.

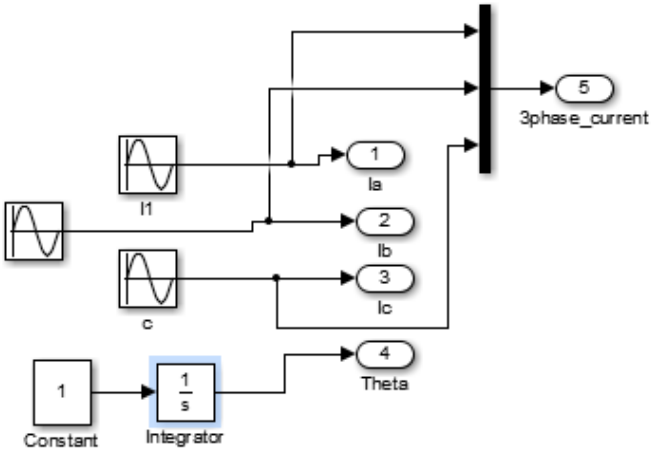

Fig. 4. Ideal sinusoidal input current

A similar block is used to model the Eq. (8) for electromagnetic torque. Figure 5 shows the flux distribution modelling.

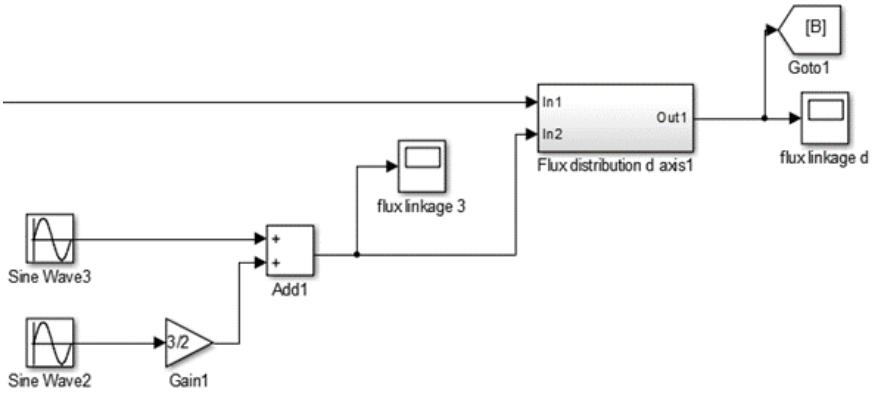

Fig. 5. Flux distribution modelling

4. Results and Discussions

4.1 ABC to D-Q Conversion

Figure 6 and 7 show the converted d-q voltage and current waveforms of TPLG-6. The d-q voltage is about 162 V and d-q current is 7.6 A.

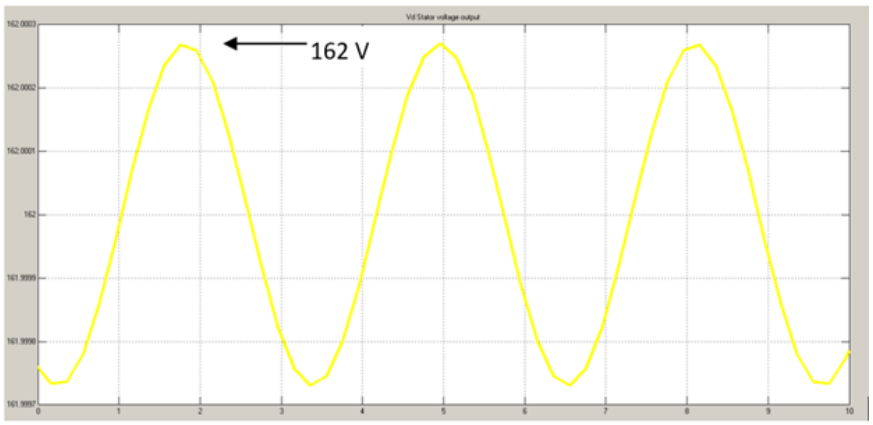

Fig. 6. D-axis voltage for TPLG-6

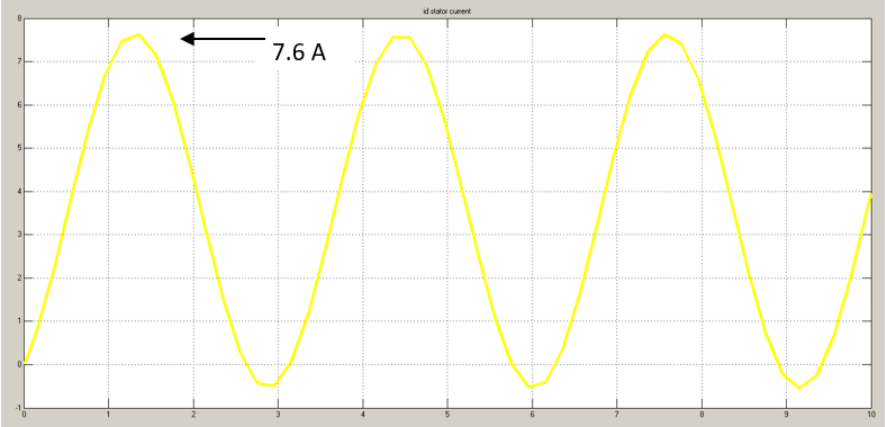

Fig. 7. D-axis current for TPLG-6

Table 1 shows the complete voltage and current results in terms of d-q axes for TPLG-6 and TPLG-18, respectively.

Table 1
D-Q current and voltage

Topologies	Parameters	*d*	*q*
TPLG-6	Voltage, V_{max}	162	5.14×10^{-4}
	Current, I_{max}, A	7.6	2
TPLG-18	Voltage, V_{max}	512	17×10^{-4}
	Current, I_{max}, A	28.6	7.7

4.2 Effect of Ld and Lq Synchronous Inductance on Permanent Magnet, (NdFeb) by Varying id and iq Current

Synchronous reactance is one of the stator components that can be studied in the following Figure 8 and 9, where the effect of synchronous inductance Ld and Lq on the permanent magnet as a translator is explained by varying the d-q current for TPLG-6. When the current in the d-axis increases, the inductance in the d-axis decreases exponentially. The q-axis inductance is similar to the d-axis but changes during the negative cycle. The flux follows the path of the d-q synchronous inductance profile and then travels through the translator corresponding to the magnetic pole. As the d-axis is drawn between the slots, it is known as the magnetising component, and the q-axis is the torque-producing component. The inductance in the d-axis is due to the flux passing between the slots, and the q-axis inductance is due to the flux passing through the translator.

Unlike asynchronous machines, flux linkage in permanent magnet machines has a lesser tendency to increase. That is one of the reasons that the q-axis, which travels through the permanent magnet translator, has a very small inductance value. Meanwhile, in the d-axis, the inductance is much greater than in the q-axis because it does not pass through the permanent magnets. Thus, the more permeable path between copper slots produces higher inductance.

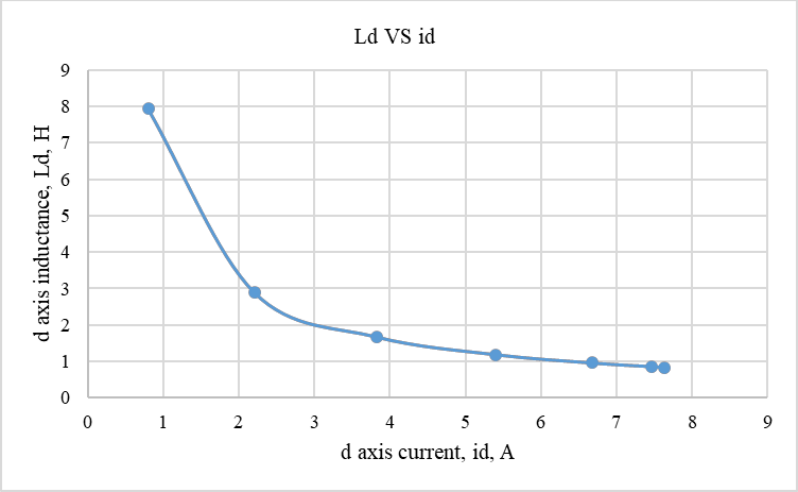

Fig. 8. D-axis Inductance for TPLG-6

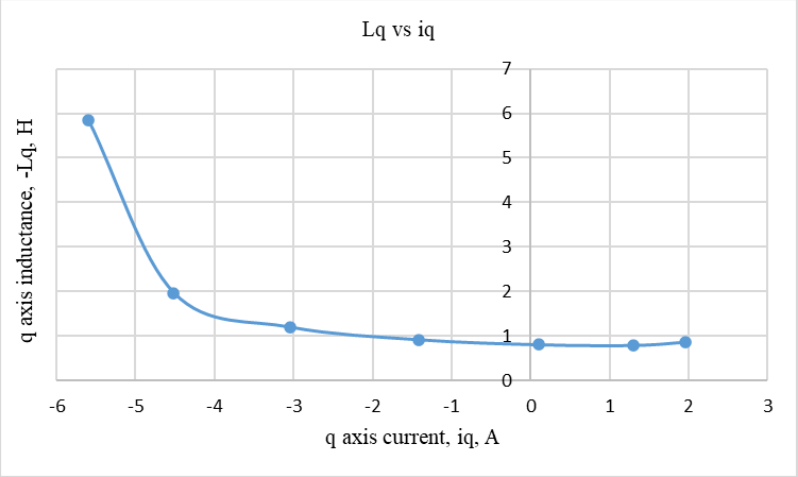

Fig. 9. Q-axis Inductance for TPLG-6

Table 2 shows the tabulated d-q inductance results that vary according to the varying d-q current.

Table 2
Current and inductance in d-q

TPLG-6	d axis current, A	d axis inductance, H	q axis current, A	q axis inductance, H
	0.806287	7.94	-5.59653	-5.83845
	2.208867	2.90	-4.51632	-1.96553
	3.823184	1.67	-3.04666	-1.19998
	5.394372	1.19	-1.4196	-0.91427
	6.674376	0.959	0.108008	-0.80068
	7.461112	0.858	1.294973	-0.78473
	7.63037	0.839	1.953903	-0.85767
TPLG-18	0.509195	48	-3.09169	-5.88
	3.032095	8.06	-9.18362	-1.98
	8.306584	2.94	-15.0425	-1.21
	14.37732	1.70	-19.7434	-0.921
	20.28588	1.20	-22.5441	-0.806
	25.09941	0.973	-23.0025	-0.790
	28.05798	0.871	-21.0461	-0.864

4.3 D-Q Power and Torque

Figure 10 and 11 show the output power waveforms of TPLG-6 and TPLG-18, respectively. The power is calculated for both d- and q-axis voltage and current.

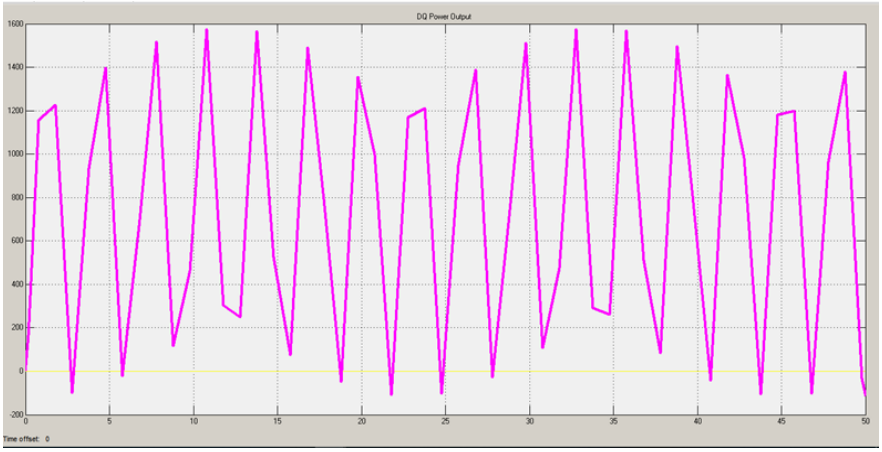

Fig. 10. Power for d-q Analysis, TPLG-6

The resulting output power appears to be distorted.

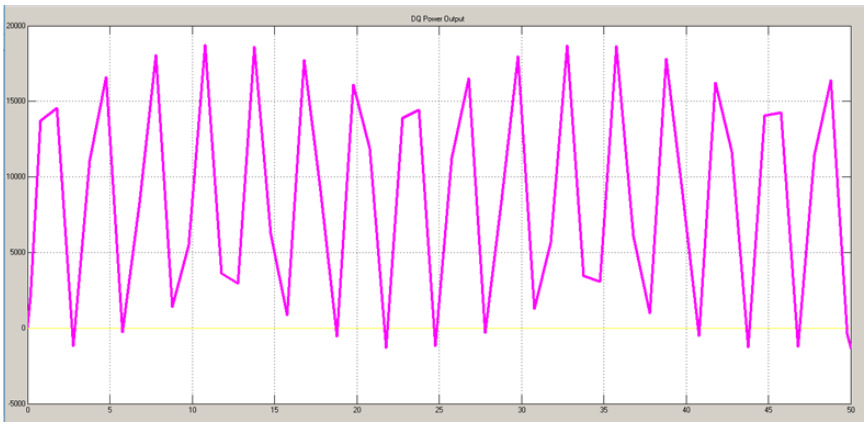

Fig. 11. Power for d-q Analysis, TPLG-18

Figure 12 and 13 depict the electromagnetic torque developed at the d-q frame for TPLG-6 and TPLG-18, respectively.

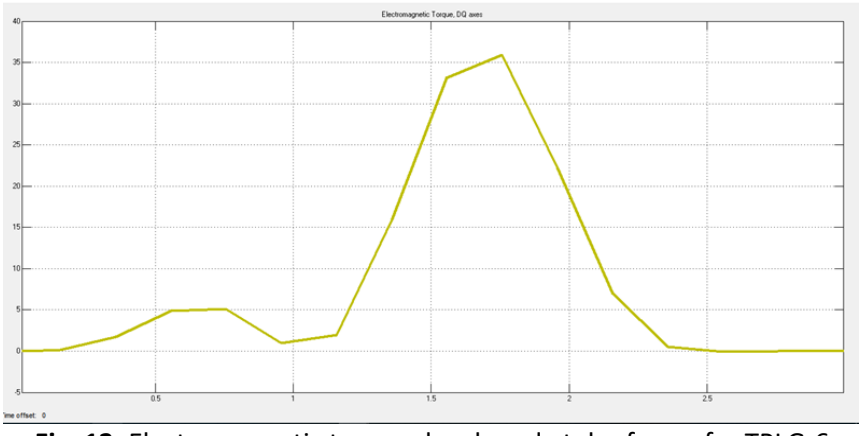

Fig. 12. Electromagnetic torque developed at d-q frame for TPLG-6

As illustrated in these figures, the torque waveforms are distorted. When the current increases, the speed increases accordingly. Therefore, the electromagnetic torque tends to drop.

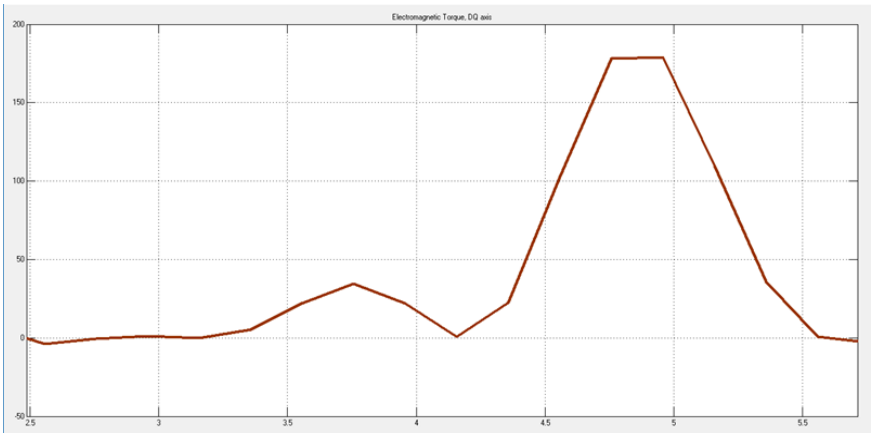

Fig. 13. Electromagnetic torque developed at d-q frame for TPLG-18

Table 3 presents the output power and torque developed for both TPLG topologies.

Table 3
Output power and torque developed

Topologies	Power,kW	$Torque_{max}$, Nm
TPLG-6	1.5	35
TPLG-18	18	187

4.4 Maximum Torque Per Ampere

The maximum Torque Per Ampere (MTPA) strategy has been implemented to study the level of torque needed for the generator to produce the maximum d-q currents at the dynamic condition. The method can reduce copper losses and improve efficiency. Graphs are plotted to find the maximum torque based on the maximum current. Figure 14 to 17 demonstrate both generators' torque behaviour as a function of d-axis and q-axis currents. It can be observed that the torque output increases steadily with the increment of the D-axis current up until a certain threshold. However, TPLG 18 consistently outperforms TPLG 6, indicating its ability to deliver higher torque levels.

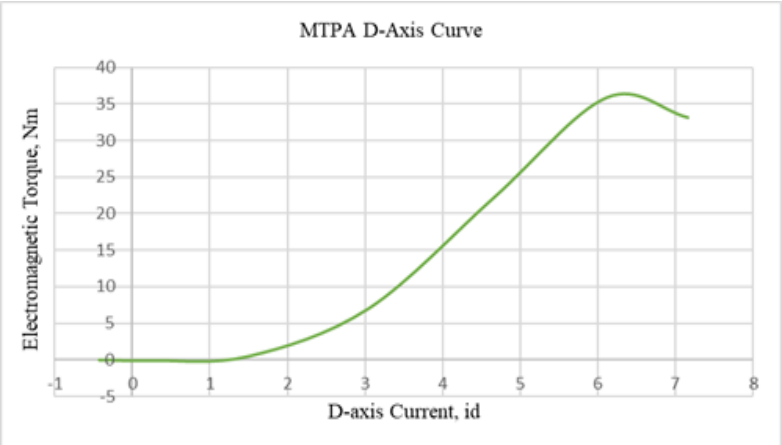

Fig. 14. Electromagnetic torque against d-axis current for TPLG-6

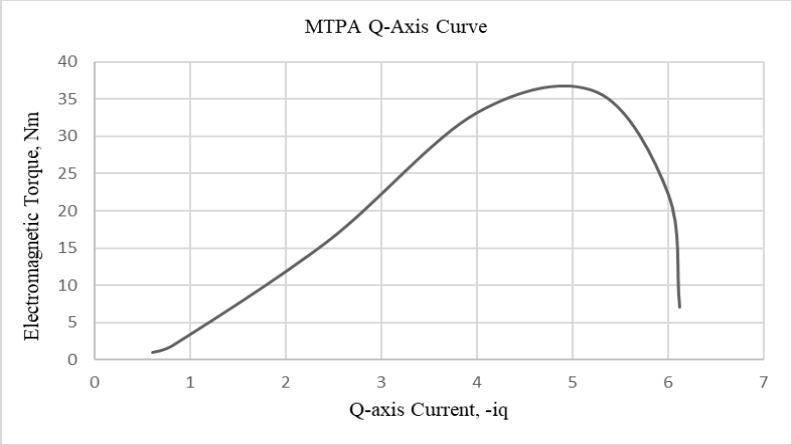

Fig. 15. Electromagnetic torque against q-axis current for TPLG-6

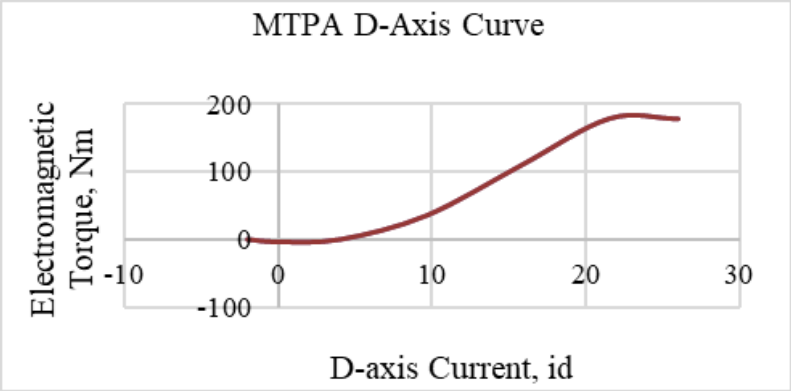

Fig. 16. Electromagnetic torque against the d-axis current for TPLG-18

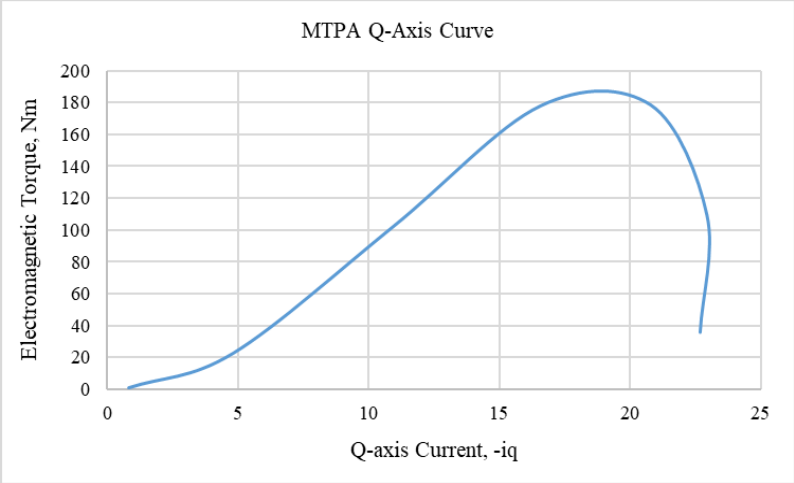

Fig. 17. Electromagnetic torque against q-axis current for TPLG-18

4.5 Saliency Ratio of L_d/L_q

Saliency is a level of quality when one parameter is relative to another. In this research, the saliency ratio explains the relationship between d-axis inductance and q-axis inductance. This ratio changes to the translator position, and maximum saliency occurs at 90 degrees of the current angle referring to the d-axis. In the salience plot against the current in both axes, id and iq show the ratio increases at the beginning and drops slowly as the current increases for TPLG-6 and a quick drop in

the ratio can be seen in the TPLG-18 ratio plot. Comparing the TPLG-6 to the TPLG-18 using a steady ratio plot reveals that the former exhibits better efficiency due to the improved performance of the permanent magnet synchronous machine caused by saliency. These are illustrated in Figure 18 and 19.

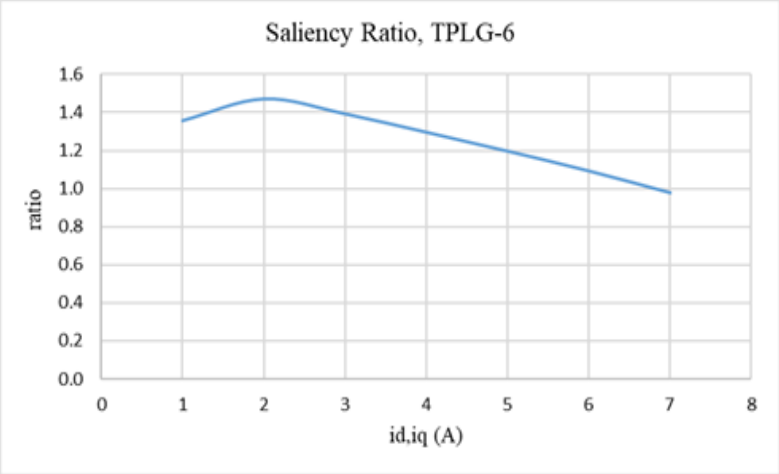

Fig. 18. Saliency ratio vs id, iq for TPLG-6

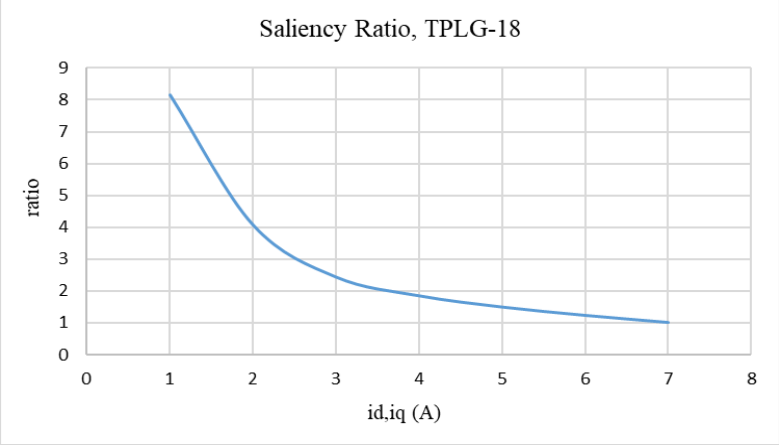

Fig. 19. Saliency ratio vs id, iq for TPLG-18

Table 4 shows the complete output of the d-q simulation when both topologies moved with a velocity of 1 ms^{-1}.

Table 4
Simulation results for d-q analysis for both topologies

Parameters	Unit	TPLG-6	TPLG-18
Average torque	Nm	22	35
Peak torque	Nm	35.8912	178.1766
Peak current	Amps	7.6	28.6
Base velocity	ms^{-1}	1	1
Average λ D	Web-t	6.5	24.4
Average λ Q	Web-t	4.7	18.2
Average λ Ld	H	1.19	1.7
Average λ Lq	H	0.91	0.92

5. Conclusions

Direct quadrature analysis is a crucial procedure in machine design. Investigating the machine parameters in a d-q frame produces more significant results and reveals the capacity of the machine and the need for further optimisation. This research has been carried out to investigate the d-q components of two topologies, namely, TPLG-6 and TPLG-18, with different design specifications but similar materials and working principles. Instead of neglecting the q-axis to have only one dc signal, q axis is included in the research since it is the torque-producing component. Since the topologies are permanent magnet synchronous machines, the rotor components need to be addressed when transforming. The ABC to DQ transformation values for both machines are almost similar to those recorded at a dynamic performance in previous research. Due to the absence of filters, great distortions are found in the resulting waveforms, which are alternating with time. The d-q inductance varies with the current where an exponential drop can be seen, which is ordinary for the d-axis inductance. Still, it has to be slightly steady for the q-axis inductance because it is a torque-producing component. The better the d-q synchronous inductance, the easier to design control systems to improve power factor and efficiency. The d-axis exhibits higher inductance because it is positioned between the slots, whereas the q-axis has lower inductance. A closer alignment between the values of Ld and Lq leads to optimal output. A greater torque is recorded to achieve maximum current in dynamic conditions due to the significant difference in Ld and Lq. The saliency ratio, on the other hand, is greater for TPLG-6 than TPLG-18. It can be concluded that TPLG-6 has greater efficiency, and TPLG-18 needs to be optimised in terms of its design specifications.

Acknowledgement
This research was not funded by any grant.

References

[1] Sinnadurai, Rajendran, C. M. Ting, and Nor Hisyam Mohd Zani. "Analysis and optimization of a three phase linear generator using Finite Element Method Magnetics (FEMM)." In *2016 IEEE Student Conference on Research and Development (SCOReD)*, pp. 1-6. IEEE, 2016. https://doi.org/10.1109/SCORED.2016.7810092

[2] Ping, Hew Wooi, and Hamzah Arof. "Design of a permanent magnet linear generator." In *2006 International Forum on Strategic Technology*, pp. 231-234. IEEE, 2006. https://doi.org/10.1109/IFOST.2006.312295

[3] Nation Master. "Malaysia_Environment Impact," (2018). https://www.nationmaster.com/country-info/profiles/Malaysia/Environment

[4] Safaai, Nor Sharliza Mohd, Zainura Zainon Noor, Haslenda Hashim, Zaini Ujang, and Juhaizah Talib. "Projection of CO2 emissions in Malaysia." *Environmental Progress & Sustainable Energy* 30, no. 4 (2011): 658-665. https://doi.org/10.1002/ep.10512

[5] Polinder, Henk, M. A. Mueller, Mattia Scuotto, and M. Goden de Sousa Prado. "Linear generator systems for wave energy conversion." In *Proceedings of the 7th European Wave and Tidal Energy Conference, Porto, Portugal*, pp. 11-14. 2007.

[6] Henderson, Ross. "Design, simulation, and testing of a novel hydraulic power take-off system for the Pelamis wave energy converter." *Renewable energy* 31, no. 2 (2006): 271-283. https://doi.org/10.1016/j.renene.2005.08.021

[7] Sinnadurai, Rajendran, C. M. Ting, and Qaslun Basheer Hadi. "A PARTICLE SWARM OPTIMIZATION APPROACH FOR THREE PHASE LINEAR GENERATOR." In *Proceedings of the Informatics Conference*, vol. 4, no. 6, pp. 1-5. 2018.

[8] Hossain, Md Jabed. "Analysis of Low Cost Permanent Magnet and Reluctance Electrical Machines with Different Rotor Anisotropy for Variable Speed Drive." (2017).

[9] Li, Jian, Zhengxing Zuo, Wenzhen Liu, Boru Jia, Huihua Feng, Wei Wang, Andrew Smallbone, and Anthony Paul Roskilly. "Generating performance of a tubular permanent magnet linear generator for application on free-piston engine generator prototype with wide-ranging operating parameters." *Energy* 278 (2023): 127851. https://doi.org/10.1016/j.energy.2023.127851

[10] Samrat, Nahidul Hoque, Norhafizan Bin Ahmad, I. A. Choudhury, and Zahari Taha. "Prospect of wave energy in Malaysia." In *2014 IEEE 8th International Power Engineering and Optimization Conference (PEOCO2014)*, pp. 127-132. IEEE, 2014. https://doi.org/10.1109/PEOCO.2014.6814412

[11] Molla, Selim, Omar Farrok, Md Rabiul Islam, and Wei Xu. "A systematic approach for designing a highly efficient linear electrical generator for harvesting oceanic wave energy." *Renewable Energy* 204 (2023): 152-165. https://doi.org/10.1016/j.renene.2023.01.020

[12] Krause, Paul C., Oleg Wasynczuk, Timothy C. O'Connell, and Maher Hasan. "Tesla's contribution to electric machine analysis." *IEEE Transactions on Energy Conversion* 32, no. 2 (2016): 591-598. https://doi.org/10.1109/TEC.2016.2640018

[13] Schmuelling, Christoph, and Stefan Kulig. "Investigation of the magnetizing inductances of the expanded park equations." In *2015 IEEE International Electric Machines & Drives Conference (IEMDC)*, pp. 357-361. IEEE, 2015. https://doi.org/10.1109/IEMDC.2015.7409084

[14] Ghazali, R. H., A. M. Ishak, SMF Syed Mohd Dardin, and AS Abu Hasim. "Characterization of Three-Phase Permanent Magnet Linear Generator for Malaysian Wave energy using Ansys Software." In *2022 IEEE International Conference on Power and Energy (PECon)*, pp. 111-116. IEEE, 2022. https://doi.org/10.1109/PECon54459.2022.9988800

[15] Li, Yang, Lei Huang, Minshuo Chen, Peiwen Tan, and Minqiang Hu. "A Linear-Rotating Axial Flux Permanent Magnet Generator for Direct Drive Wave Energy Conversion." In *2021 13th International Symposium on Linear Drives for Industry Applications (LDIA)*, pp. 1-4. IEEE, 2021. https://doi.org/10.1109/LDIA49489.2021.9505815

[16] Sinnadurai, Rajendran, Devika Sethu, and Muhammad Firdaus Hairulizam. "Simulating a Sea Wave Power Plant for Malaysia." *Journal of Advanced Research in Applied Sciences and Engineering Technology* 30, no. 1 (2023): 90-104. https://doi.org/10.37934/araset.30.1.90104

[17] Yaakob, Yusli, Mahamad Hisyam Mahamad Basri, Muhammad Farhan Bardzan, Noor Iswadi Ismail, Azli Abd Razak, and Muhammad Arif Ab Hamid Pahmi. "The Stability Analysis Of Floating Buoy As A Wave Energy Harvester For Malaysian Coastal Area." *Journal of Advanced Research in Applied Mechanics* 96, no. 1 (2022): 1-6. https://doi.org/10.37934/aram.96.1.16

[18] Samsudin, Muhammad Syazwan Nizam, Md Mizanur Rahman, and Muhamad Azhari Wahid. "Sustainable power generation pathways in Malaysia: Development of long-range scenarios." *Journal of Advanced Research in Applied Mechanics* 24, no. 1 (2016): 22-38.

[19] Muhammadu, Masin Muhammadu, and Jafuru Usman. "Small hydropower development in North-Central of Nigeria: An assessment." (2014).

[20] Liang, Vernon Yeoh Sheng, Nur Irwany Ahmad, Diyya Hidayah Abd Rahman, Aimi Athirah, Hazwani Zaidi, Saidatul Shema Saad, Nazrul Azril Nazlan, Habibah Mokhtaruddin, and Baseemah Mat Jalaluddin. "Development of Solar Tracking Robot for Improving Solar Photovoltaic (PV) Module Efficiency." *Journal of Advanced Research in Applied Mechanics* 61 (2019): 13-24.